Exciton-correlated hole tunneling in mixed-type GaAs quantum wells

Thomas K. Baldwin,[1] Stephen A. McGill,[2] and Hailin Wang[1]
[1]*Department of Physics, University of Oregon, Eugene, Oregon 97403, USA*
[2]*National High Magnetic Field Laboratory, 1800 East Paul Dirac Drive, Tallahassee, Florida 32310, USA*
(Received 16 February 2014; revised manuscript received 18 June 2014; published 11 July 2014)

We report an experimental study on the tunneling of holes in a mixed-type GaAs quantum-well structure, in which an electron-hole bilayer forms through optical carrier injection. In this bilayer system, an interlayer correlation between holes and excitons can strongly enhance the hole tunneling rate, opening a new avenue for optical control of transport processes in semiconductors. Interlayer hole tunneling is characterized with respect to these excitonic correlations, as well as carrier densities, temperature, and magnetic field, providing valuable insights on the tunneling process.

DOI: 10.1103/PhysRevB.90.035304 PACS number(s): 73.40.Gk, 71.35.Gg, 71.35.Ji, 78.67.−n

I. INTRODUCTION

In a bilayer system, electrons and holes are separated by a thin barrier. These systems are of interest as a platform for studying the collective behavior of excitons since the physical separation of carriers leads to longer exciton lifetimes [1,2]. Cross-layer Coulomb potentials can be manipulated to create artificial lattices [3], while interlayer correlations between carriers can lead to other subtle behaviors, as shown by recent studies on the Kondo effect [4] and biexciton formation [5]. In particular, the tunneling of the electrons or holes across the barrier can depend on the interlayer Coulomb correlation between the carriers. As beautifully demonstrated in an earlier experimental study on bilayers formed in modulation-doped GaAs quantum wells (QWs) in the quantum Hall regime, a giant increase in the tunneling rate occurs when every electron is positioned opposite a hole across the barrier [6]. This giant increase in the tunneling rate was also taken as evidence for the Bose-Einstein condensation of the electron-hole pairs in the bilayer system [7].

In this paper, we report an experimental study on the tunneling of holes in an electron-hole bilayer system formed in a GaAs mixed-type quantum well (MTQW). Detailed experimental studies have investigated the dependence of the hole tunneling rates on temperature, carrier density, exciton density, and external magnetic fields. These studies reveal, surprisingly, that a correlation between holes and excitons across the barrier can strongly enhance the hole tunneling rate. Tunneling, which is a fundamental quantum process and is important for many device applications, is generally viewed as a single-particle transport process [8–10]. Correlation-enhanced tunneling due to the Coulomb interaction between the holes and excitons couples together optical and transport processes, thus providing an avenue for optical manipulation of transport processes in semiconductors.

In a GaAs MTQW, a narrow GaAs well is separated by a thin AlAs barrier from a wide GaAs well (see Fig. 1). The narrow well (NW) is a type-II QW, in which quantum confinement raises the bottom of the conduction band higher in energy than the X valley in the AlAs barrier. After an optical excitation of electron-hole pairs in the NW, electrons can transfer via the X valley in the barrier to the conduction band of the wide well (WW), while the holes remain trapped in the NW [11,12]. Carrier densities ranging from $10^7/\text{cm}^2$ to $10^{10}/\text{cm}^2$ can be generated and controlled via the optical excitation. The excess electrons and holes separated by the thin barrier form an electron-hole bilayer, with the lifetime of the carriers determined by the tunneling of the holes from the narrow to the wide well [13,14]. Excitonic properties of MTQWs have also been extensively investigated [15–23]. In contrast to the bilayer system formed in modulation-doped QWs, the electron-hole bilayer in a MTQW can be generated, manipulated, and probed all with optical techniques.

II. SAMPLES AND EXPERIMENTAL SETUP

The sample used in our studies consists of three periods of narrow (2.5 nm) and wide (16 nm) GaAs wells separated by

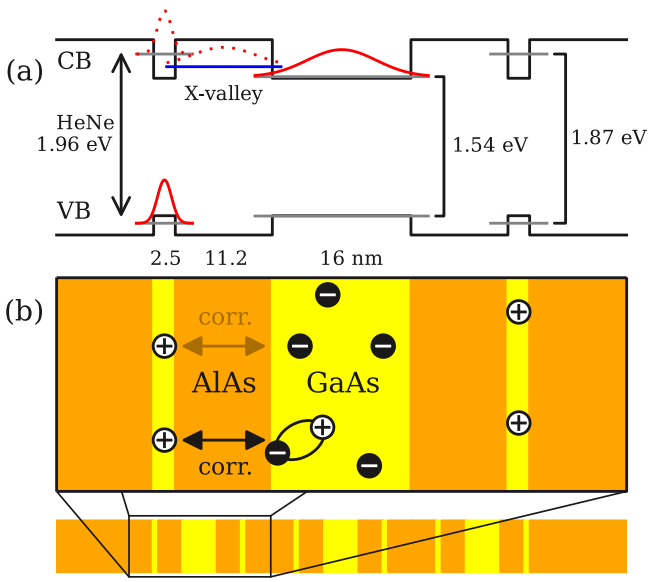

FIG. 1. (Color online) (a) Band-edge profile of a MTQW. A HeNe laser (1.96 eV) excites electrons from the valence band (VB) to the conduction band (CB) of the NW. The electrons relax to the lower energy WW via an intermediary state in the X valley of the barrier, while the holes remain trapped in the NW. (b) Schematic illustrating interlayer Coulomb correlations between NW holes and WW excitons. These correlations can lead to accelerated hole tunneling.

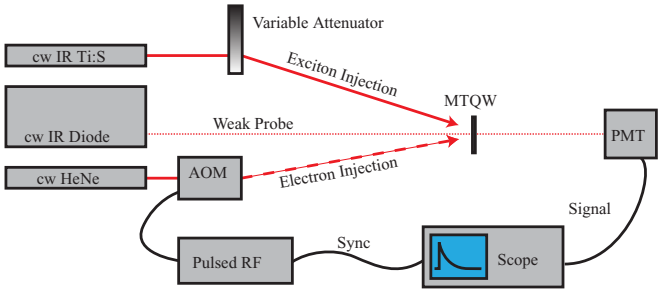

FIG. 2. (Color online) Experimental configuration for tunneling measurements. A continuous-wave infrared (cw IR) diode laser serves as a probe to monitor sample transmission at the HH exciton resonance, while a HeNe laser, gated by an acousto-optic modulator (AOM), periodically injects electrons to the WW from the NW. For studies involving exciton injection, a third beam (a cw Ti:sapphire laser) was added at the LH exciton resonance. PMT: photomultiplier tube.

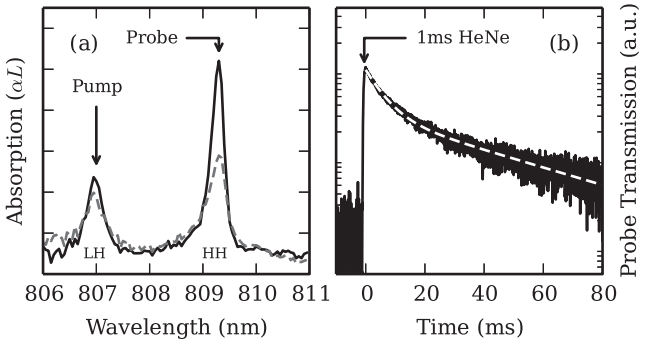

FIG. 3. (a) Absorption spectrum showing wide-well HH and LH exciton resonances (solid lines) at 10 K. A continuous-wave HeNe laser with an intensity of 0.1 mW/cm^2 injects an electron gas, which bleaches the exciton resonances (dashed lines). (b) Time-resolved optical transmission at the HH exciton line in response to a 1-ms pulsed HeNe excitation of 5 mW/cm^2. Decay is well described by a double-exponential function (dashed line).

an 11.2-nm AlAs barrier, as illustrated in Fig. 1. Two NWs have been placed symmetrically on both sides of the WWs in order to minimize space-charge fields due to buildup of spatially separated carriers. For the formation of an electron-hole bilayer, a HeNe laser ($\lambda = 633$ nm) excites electron-hole pairs in the NW, generating long-lived excess electrons in the WW and holes in the NW. The HeNe laser spot was chosen to be larger than the sample to guarantee a spatially uniform distribution of injected carriers.

These excess electrons broaden and bleach the WW exciton absorption resonances [22,24]. Since the rate of hole tunneling determines the recovery time of the exciton absorption line, we can measure the hole tunneling rate by monitoring optical transmission at an exciton absorption peak following the injection of electrons into the WW by a HeNe laser pulse.

The experimental configuration for transient optical studies is shown schematically in Fig. 2. HeNe laser pulses are generated by gating a continuous-wave (cw) HeNe laser with an acousto-optic modulator. We probe the rate of hole tunneling using a weak cw probe beam tuned to the heavy-hole (HH) exciton resonance. For experiments investigating the dependence of the hole tunneling rate on the density of excitons, a separate cw pump tuned to the light-hole (LH) exciton resonance is used to inject LH excitons directly to the WW. These excitons relax to HH excitons on a time scale of a few picoseconds.

Unless otherwise specified, all experiments were performed with the sample held at 10 K in a helium flow cryostat. Magnetic field dependence was studied using the 25T Split Florida-Helix resistive magnet at the National High Magnetic Field Laboratory in Tallahassee, Florida.

III. RESULTS

We have carried out detailed experimental studies to probe the interlayer tunneling of the holes in the MTQW sample. These investigations are grouped according to whether exciton injection was used in the experiment. Results obtained without the exciton injection help characterize how the QW energy-level structure influences the tunneling process, while experiments involving the exciton injection probe the effects of interlayer as well as intralayer Coulomb correlations on the tunneling process.

A. Tunneling in the absence of exciton injection

Results of a typical tunneling measurement are shown in Fig. 3. Figure 3(a) shows the bleaching of the HH exciton resonance by the injection of electrons into the WW. No shift in the absorption lines is observed that would imply a buildup of charges outside the well structure. Figure 3(b) plots the time-resolved recovery of the HH exciton absorption resonance shown in Fig. 3(a). This recovery reflects the decay of excess electron population in the WW, which results from interlayer tunneling of the holes followed by radiative recombination. The decay of the electron population shown in Fig. 3(b) is double exponential in nature, characterized by a fast component with a decay time of several milliseconds and a slow component with a decay time of tens of milliseconds. Since the electron-hole or exciton recombination time (on the order of nanoseconds) is orders of magnitude faster than the hole tunneling time, the decay of the electron population shown in Fig. 3(b) measures directly the interlayer tunneling rate of the holes.

Figure 4(a) shows the dependence of the fast and slow hole tunneling rates on the excess electron density in the WW, controlled here by the intensity of the HeNe laser. A HeNe pulse, with a duration of 1 ms and with a peak intensity of 4 mW/cm^2, is estimated to inject on the order of a few times 10^9 electrons/cm^2 to the WW [17,23]. As shown in Fig. 4(a), the tunneling rates are largely insensitive to the electron density when the HeNe laser intensity exceeds 3 mW/cm^2. This indicates that, within this range, the buildup of space-charge fields associated with the injected electron population does not affect the measurement. For the rest of the tunneling experiments presented in this paper, the experiments were performed at sufficiently high electron densities such that the tunneling rates are nearly independent of the electron density.

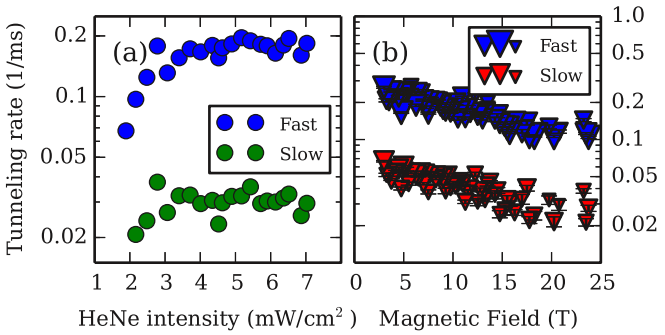

FIG. 4. (Color online) (a) Extracted hole tunneling rates as a function of electron density, as controlled by the peak intensity of a 1-ms HeNe laser pulse. (b) Dependence of the hole tunneling rates on magnetic field. A 1-ms HeNe laser pulse with a peak intensity of 4 mW/cm^2 was used.

Figure 4(b) shows the dependence of the hole tunneling rate on the magnitude of a magnetic field applied perpendicular to the QW. The tunneling rates decrease monotonically with the increasing magnetic field.

B. Hole tunneling involving WW excitons

The injection of a dilute gas of excitons to the WW can lead to a substantial increase in the hole tunneling rate. This exciton-correlated tunneling effect can lead to a counterintuitive optical response, such as the excitation-induced exciton absorption reported in an earlier experimental study [23].

For a detailed study of the exciton-correlated tunneling, a cw pump beam was tuned to the LH exciton resonance during the tunneling measurement, injecting a variable density of excitons to the WW. The inset of Fig. 5 shows an example of time-resolved transmission at the HH resonance with and without the pump beam. As shown in Fig. 5, the exciton injection enhances the tunneling of the holes. The pump intensity used in the experiment is 0.2 W/cm^2, corresponding to an estimated exciton density on the order of 10^8/cm^2.

Figure 5 shows the dependence of the hole tunneling rate on the pump intensity obtained at various temperatures. At lower temperatures, the tunneling rate is slower and more sensitive to the enhancement induced by the exciton correlation. At 5 K, the rate can be made 12 times faster by applying a pump 100 mW/cm^2 in intensity, whereas at 15 K the rate may only be made twice as fast. Note that the enhancement in the tunneling rate levels off when the pump beam reaches a modest intensity of 0.1 W/cm^2.

To get a better understanding of the exciton-correlation-induced hole tunneling, we have also carried out experimental studies in the presence of a high magnetic field (5 to 20 T) perpendicular to the QW plane (see Fig. 6). Under these magnetic fields, the hole tunneling rate becomes nearly independent of the injection of excitons in the WW. The strong magnetic field effectively quenches the enhanced hole tunneling induced by the exciton injection in the WW.

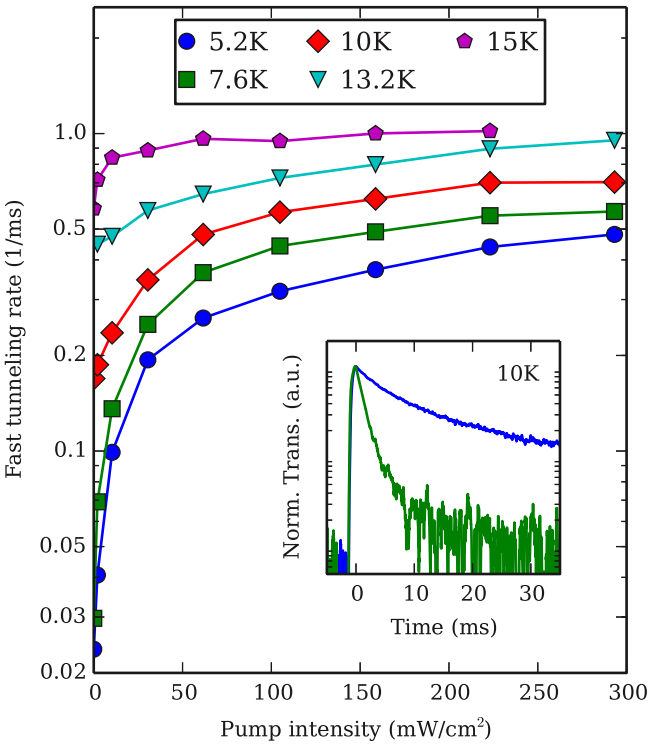

FIG. 5. (Color online) Hole tunneling rate (fast component) on a logarithmic scale as a function of pump intensity. At high exciton densities, the hole tunneling rate is accelerated. This effect is more pronounced at lower temperatures. Inset: Time-resolved transmission at the heavy-hole exciton resonance of the WW in the presence of a HeNe laser pulse 1 ms in duration and 5 mW/cm^2 in peak intensity. Hole tunneling is accelerated in the presence of a cw pump beam with an intensity of 0.2 W/cm^2 at the LH exciton (green line) relative to without exciton pumping (blue line). Vertical scale is logarithmic.

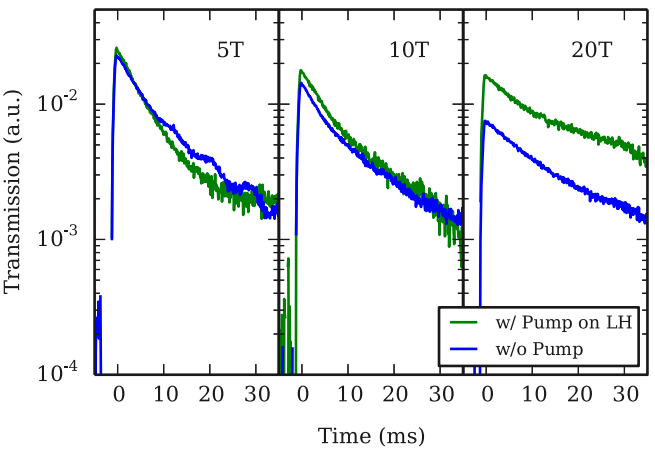

FIG. 6. (Color online) Time-resolved transmission at the heavy-hole exciton resonance of the WW at 10 K, in response to a 1-ms HeNe pulse with a peak intensity of 4 mW/cm^2. Experiment performed at 10 K in the presence (green lines) and absence (blue lines) of a 100 mW/cm^2 exciton injection beam tuned to the LH exciton resonance in various perpendicular magnetic fields. The tunneling rate enhancement evident in Fig. 5(a) is not observed at these magnetic fields.

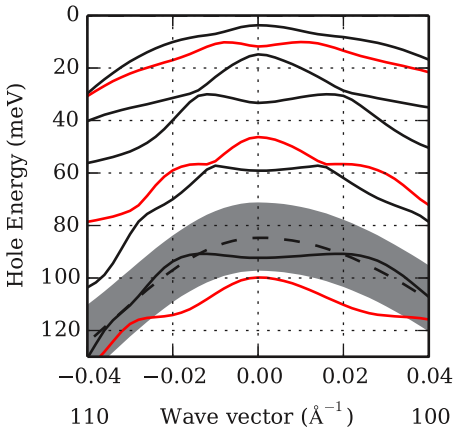

FIG. 7. (Color online) Calculated subband dispersion for narrow (dashed lines) and wide (solid lines) wells. Red lines indicate LH bands; other lines indicate HH. Tunneling occurs where the ground NW state and the fifth excited WW HH state overlap. The gray band indicates the energetic difference made by monolayer fluctuations in the NW.

IV. DISCUSSION

The hole tunneling depends on the relevant energy levels of the MTQW. Figure 7 shows the valence-band energy-level structures of both NW and WW (see Ref. [23] for details of the theoretical calculation). As indicated in Fig. 7, the lowest-energy HH valence band (HH1) in the NW is energetically close to the the fifth HH valence band (HH5) in the WW. The hole tunneling process must satisfy energy and momentum conservation. The tunneling can take place where valence subbands of the two wells cross in Fig. 7 [14], or can occur through a phonon-assisted process.

It is well known that well-width fluctuations in a QW lead to an inhomogeneous broadening of the QW energy levels. A width fluctuation of one monolayer induces a much greater energy variation in the NW than that in the WW [25]. We estimate that NW bands are inhomogenously broadened by up to 10 meV, as illustrated by the gray band in Fig. 7. Holes in the NW are expected to be thermally distributed in the HH1 band within this spectral range, overlapping to varying degrees with the HH5 band of the WW. Note that these holes are spatially localized by the fluctuations in the confinement potential [25].

The double-exponential character of the tunneling curve in Fig. 3(b) can be attributed to this inhomogeneous distribution of the holes in the NW. Specifically, we associate the slow decay component with the holes at the bottom of the thermal distribution. Absorption of phonons with a relatively large energy to compensate the energy between the relevant HH5 and HH1 bands is needed in order for the tunneling process to take place. Conversely, the fast component is associated with holes that are near the higher-energy region of the inhomogeneous distribution, which nearly overlaps with the HH5 band in the WW. This interpretation is supported by our earlier experimental study, which shows that at relatively low temperatures ($T < 30$ K), the fast tunneling rate depends more sensitively on the temperature than the slow tunneling rate does [23].

The flat dependence of the hole tunneling rate on the HeNe laser intensity shown in Fig. 4(a) indicates that shifts in the subband alignment due to electric fields associated with the electron-hole separation are small. The falloff at low intensity can be understood in a way similar to the temperature dependence since the lower-energy states in the HH1 are expected to fill prior to the higher-energy states associated with the fast tunneling rate. At these low densities the tunneling curve would be better described by a single exponential at the slow rate.

In the presence of a magnetic field perpendicular to the QW plane, both the electron and hole energy levels in the QW are quantized into discrete Landau levels. However, even at the highest magnetic field used, the quantization energy (∼2 meV at 20 T for electrons, estimated from $E = \hbar eB/m_e$) is still small compared with the large inhomogeneous broadening of the NW hole bands. As shown in Fig. 4(b), the magnetic field leads to a gradual decrease in the tunneling rate with increasing magnetic field, a result consistent with prior studies on interwell tunneling [26]. Although the magnetic field leads to no qualitative changes in the overall behavior of the hole tunneling, it does lead to major changes in how the exciton injection in the WW affects the hole tunneling rate, as will be discussed in detail later.

With this understanding of the link between the hole tunneling rates and the valence-band energy-level structures, we now proceed to discuss how the presence of excitons in the WW affects the tunneling of the holes in the NW. It is well known that both negatively and positively charged excitons (trions) can form in GaAs QWs [27]. For the positively charged exciton, a hole is bound to an exciton. In a MTQW, the presence of the 11.2-nm barrier prevents binding of NW holes to WW excitons, but there still exist Coulomb correlations between the two, as shown schematically by the dark correlation arrow in Fig. 1(b). This correlation can be substantial when the hole lies opposite the exciton across the barrier, lowering the potential barrier and leading to faster hole tunneling processes. This is to some extent similar to the tunneling process observed in an electron-hole bilayer system in the quantum Hall regime, where an electron positioned directly opposite a hole in a bilayer can greatly enhance the tunneling process [6,7].

With the evidence of interlayer exciton-hole correlation, a question naturally arises as to why there is no evidence of interlayer correlations between electrons and holes in the MTQW. This "missing" correlation is shown by the weak correlation arrow in Fig. 1(b). With a sufficiently thin barrier, interlayer correlations between electrons and holes lead to the formation of indirect excitons, as shown in extensive studies [2,28]. Using the method in Ref. [29], we estimate the binding energy for indirect excitons in our sample to be ∼1 meV or smaller, and we have not observed them in experiments. The electron-hole correlation is weak unless the electron in the WW is directly opposite to or at least near the hole in the NW, which is unlikely under our experimental condition (at $T = 10$ K and with relatively high mobility for the electrons in the WW). The relatively strong interlayer exciton-hole correlation is due in large part to the fact that the interface roughness inherent in a QW leads to relatively small exciton mobility, or ambipolar diffusion coefficient [30–32]. In essence, excitons are much heavier than the electrons and thus are much less mobile

amid the interface potential fluctuations. Hence, exciton-hole correlations are more evident than electron-hole correlations by virtue of their longer interaction time.

The enhanced tunneling arising from exciton injection is not due to heating induced by the optical excitation. First of all, the exciton density involved in these experiments is relatively low, less than $10^8/\text{cm}^2$, at which the heating should be negligible. This is further confirmed by the experimental results shown in Fig. 5. Most of the increase in the tunneling is observed at the lowest exciton densities. Furthermore, the enhancement levels off at relatively high exciton densities, and the maximally accelerated tunneling rate is a function of the temperature. Note that the results of Fig. 5 show that while the hole tunneling rate is faster with increasing temperature, the degree of enhancement by the exciton correlations (indicated by the vertical range spanned by the traces) is reduced with increasing temperature, a finding consistent with the temperature dependence of analogous correlation effects described in the quantum Hall experiments [7].

The quenching of exciton-correlation-enhanced tunneling by a strong magnetic field shown in Fig. 6 provides additional physical insights into the interlayer Coulomb correlation, especially on the important role of exciton mobility. As shown in an earlier experimental study on the diffusion coefficient of excitons in the presence of a magnetic field, the exciton mobility decreases quickly with increasing field [33]. At the relatively high magnetic field used in Fig. 6, the excitons are effectively localized such that, within the short nanosecond lifetime, they cannot migrate to regions that are opposite to or near holes in the NW. In this regard, the magnetic freeze-out of the excitons effectively quenches the interlayer Coulomb correlation between the holes in the NW and the excitons in the WW.

V. CONCLUSION

In summary, experimental studies of hole tunneling in a MTQW show that the tunneling process depends sensitively on the energy-level structures of the valence band in both narrow and wide quantum wells of the MTQW. The dependence of the tunneling process on the excitonic excitation in the wide quantum well also provides evidence that there can be strong correlations between holes in the narrow quantum well and excitons in the wide quantum well. These Coulomb correlations lead to enhanced hole tunneling. The exciton-correlation-enhanced tunneling can provide a mechanism for using optical excitations to manipulate tunneling processes, thus enabling optical control of transport processes.

ACKNOWLEDGMENTS

We thank J. Prineas for providing the MTQW samples used in our experimental studies and C. Phelps for performing the theoretical calculation on the valence-band energy-level structures of the MTQW. J. Garman and D. Semenov provided technical services and support. This work is supported by the NSF under Grant No. DMR-1104718. Portions of the work were conducted at the National High Magnetic Field Laboratory, which is supported by the NSF through NSF Grant No. DMR-0084173 and by the state of Florida.

[1] A. A. High, J. R. Leonard, A. T. Hammack, M. M. Fogler, L. V. Butov, A. V. Kavokin, K. L. Campman, and A. C. Gossard, Nature (London) **483**, 584 (2012).
[2] D. W. Snoke, Adv. Condens. Matter Phys. **2011**, 938609 (2011).
[3] M. Remeika, J. C. Graves, A. T. Hammack, A. D. Meyertholen, M. M. Fogler, L. V. Butov, M. Hanson, and A. C. Gossard, Phys. Rev. Lett. **102**, 186803 (2009).
[4] C. Latta, F. Haupt, M. Hanl, A. Weichselbaum, M. Claassen, W. Wuester, P. Fallahi, S. Faelt, L. Glazman, J. von Delft, H. E. Tureci, and A. Imamoglu, Nature (London) **474**, 627 (2011).
[5] C. Schindler and R. Zimmermann, Phys. Rev. B **78**, 045313 (2008).
[6] I. B. Spielman, J. P. Eisenstein, L. N. Pfeiffer, and K. W. West, Phys. Rev. Lett. **84**, 5808 (2000).
[7] J. P. Eisenstein and A. H. MacDonald, Nature (London) **432**, 691 (2004).
[8] D. J. Griffiths, *Introduction to Quantum Mechanics*, 2nd ed. (Pearson Prentice Hall, Upper Saddle River, NJ, 2005).
[9] L. L. Chang, L. Esaki, and R. Tsu, Appl. Phys. Lett. **24**, 593 (1974).
[10] E. E. Mendez, W. I. Wang, B. Ricco, and L. Esaki, Appl. Phys. Lett. **47**, 415 (1985).
[11] I. Galbraith, P. Dawson, and C. T. Foxon, Phys. Rev. B **45**, 13499 (1992).
[12] P. Dawson, I. Galbraith, A. I. Kucharska, and C. T. Foxon, Appl. Phys. Lett. **58**, 2889 (1991).
[13] P. Dawson and M. J. Godfrey, Phys. Rev. B **68**, 115326 (2003).
[14] A. M. Malik, M. J. Godfrey, and P. Dawson, Phys. Rev. B **59**, 2861 (1999).
[15] A. Ron, H. Yoon, M. Sturge, A. Manassen, E. Cohen, and L. Pfeiffer, Solid State Commun. **97**, 741 (1996).
[16] A. Manassen, E. Cohen, A. Ron, E. Linder, and L. N. Pfeiffer, Phys. Rev. B **54**, 10609 (1996).
[17] H. W. Yoon, A. Ron, M. D. Sturge, and L. N. Pfeiffer, Solid State Commun. **100**, 743 (1996).
[18] M. Kozhevnikov, E. Cohen, A. Ron, H. Shtrikman, and L. N. Pfeiffer, Phys. Rev. B **56**, 2044 (1997).
[19] A. Nazimov, E. Cohen, A. Ron, E. Linder, H. Shtrikman, and L. Pfeiffer, Physica E (Amsterdam, Neth.) **6**, 650 (2000).
[20] R. Rapaport, R. Harel, E. Cohen, A. Ron, E. Linder, and L. Pfeiffer, Phys. Status Solidi A **178**, 481 (2000).
[21] T. Yeo, B. D. McCombe, B. M. Ashkinadze, and L. Pfeiffer, Physica E (Amsterdam, Neth.) **12**, 620 (2002).
[22] M. Koch, R. Hellmann, G. Bastian, J. Feldmann, E. O. Göbel, and P. Dawson, Phys. Rev. B **51**, 13887 (1995).
[23] C. Phelps, J. Prineas, and H. Wang, Phys. Rev. B **83**, 153302 (2011).
[24] S. Schmitt-Rink, D. Chemla, and D. Miller, Adv. Phys. **38**, 89 (1989).
[25] D. Gammon, E. S. Snow, B. V. Shanabrook, D. S. Katzer, and D. Park, Phys. Rev. Lett. **76**, 3005 (1996).

[26] S. Denev, V. Negoita, D. W. Snoke, B. Laikhtman, K. Eberl, and L. Pfeiffer, Phys. Rev. B **66**, 205304 (2002).
[27] G. Finkelstein, H. Shtrikman, and I. Bar-Joseph, Phys. Rev. Lett. **74**, 976 (1995).
[28] L. V. Butov, J. Phys. Condens. Matter **16**, R1577 (2004).
[29] K. Sivalertporn, L. Mouchliadis, A. L. Ivanov, R. Philp, and E. A. Muljarov, Phys. Rev. B **85**, 045207 (2012).
[30] J. Hegarty, L. Goldner, and M. D. Sturge, Phys. Rev. B **30**, 7346 (1984).
[31] H. Wang, M. Jiang, and D. G. Steel, Phys. Rev. Lett. **65**, 1255 (1990).
[32] H. Tang, J. Phys. Condens. Matter **15**, 8137 (2003).
[33] M. Jiang, H. Wang, R. Merlin, D. G. Steel, and M. Cardona, Phys. Rev. B **48**, 15476 (1993).